Characterizing Spatiotemporal Pattern of Vegetation Greenness Breakpoints on Tibetan Plateau Using GIMMS NDVI3g Dataset

YONG NI[1,2,3], YUKE ZHOU[ID][4], AND JUNFU FAN[ID][5]

[1]State Key Laboratory of Resources and Environmental Information System, Institute of Geographic Science and Natural Resources Research, Chinese Academy of Sciences, Beijing 100101, China
[2]College of Resources and Environment, University of Chinese Academy of Sciences, Beijing 100049, China
[3]China National Environmental Monitoring Center, Beijing 100012, China
[4]Key Laboratory of Ecosystem Network Observation and Modeling, Institute of Geographic Sciences and Natural Resources Research, Chinese Academy of Sciences, Beijing 100101, China
[5]School of Civil and Architectural Engineering, Shandong University of Technology, Zibo 255049, China

Corresponding authors: Yuke Zhou (zhouyk@igsnrr.ac.cn) and Junfu Fan (fanjf@sdut.edu.cn)

ABSTRACT Due to the harsh natural environment on the Tibetan Plateau (TP), its vegetation is sensitive to climate change. Therefore, it is essential to characterize long-term vegetation shifts for understanding of land surface processes across the TP. Gradual greening or browning growth in vegetation greenness is detectable while the alternating process between greening and browning, its timing, and type remain unclear. In this paper, breakpoint in time series of a satellite-derived vegetation index was detected at pixel-level during 1982-2012. The long-term growth procedure of vegetation was then characterized by combining the greening/browning trend for the two sub-periods, on each side of the breakpoint. The combinations of greening/browning status were classified into three categories (monotonic, interrupted and growth reversal). Possible causes for abrupt vegetation changes are discussed in the content of climate change and grassland management. Results show that breakpoints are temporally widely distributed and have significant spatial heterogeneity. About 21% (11%) of the vegetated area showed significant greening (browning) trends. Vegetation in central and eastern TP has tended to be greening. Browning trends were particularly evident in the southern and northeastern TP and were scarce in the west. About 32% of the vegetation was found to change significantly in this analysis. Greening trends occurred more often than browning trends and exhibited both a monotonic and an interrupted growing process. Trend reversal in vegetation was dominated by declining trends. Breakpoints in monotonic and interrupted trends were concentrated in some time points, but those with reversal trends were discretely distributed over time span. Among different ecosystem types, desert ecosystems presented the most significant greening trends, accounting for 53% of plant-covered desert. Conspicuous degraded trends were identified on alpine sparse vegetated area. Statistically, breakpoints in precipitation and air temperature are not consistent with those in vegetation greenness index. And grazing projects have not posed a significant effect on abrupt shifts in vegetation greenness.

INDEX TERMS Tibetan Plateau (TP), greening and browning, breakpoints, seasonal-trend model, GIMMS NDVI3g.

I. INTRODUCTION

Vegetation plays an essential role in the exchange of carbon, water, and energy between land surface and atmosphere [1]–[3], and it is essential to examine long-term

The associate editor coordinating the review of this manuscript and approving it for publication was Xian Sun[ID].

changes and interannual variability from regional to global scales, particularly in fragile ecosystems. These trends and variability have been used extensively for terrestrial ecosystem monitoring, especially for assessing ecological responses to carbon cycle dynamics [4], land cover changes [5], and various ecosystem shifts. In addition to these trends, commonly analyzed linearly, abrupt changes in long-term

vegetation data occur. These changes have not been fully identified even though they can reveal interactions between plants and environmental changes [1], [6].

The Tibetan Plateau (TP) is sensitive to global climate change, as a result of its elevation (approximately 4000 m above sea level) [7], [8]. For instance, temperature on the TP has been increasing at a much faster rate than in all of China and other parts of eastern Asia [9]. In fact, the TP has become an ideal place for assessing vegetation dynamics and vegetation's relationship with pedospheric, atmospheric, and hydrospheric systems [10], [11]. Due to its capability to measure chlorophyll and energy absorption, the Normalized Difference Vegetation Index (NDVI) has been applied extensively as a proxy for a number of vegetative biophysical parameters, including biomass and productivity [12], [13]. Recently, the release of the longest NDVI time series to date - GIMMS NDVI3g - enables us to perform long-term analyses for interannual variation in NDVI and its relationship to temperature and precipitation throughout the TP [14]. Vegetation across the TP has demonstrated an obvious greening trend due to both substantially increased growth and a prolonged growing season length [15]. This is consistent with similar findings at the global scale that most of the northern ecosystems are becoming greener, with some browning regions at high latitudes in North America and central Eurasia[1], [4], [16]–[20]. Since the beginning of the 1980s, vegetation on the TP has been greening in general, although there are significant regional and seasonal differences in vegetation status [21], [22]. Guo et al., examined the greenness trend of grasslands on the plateau using MODIS images and found a significant increase in NDVI, primarily in the northeastern TP. Significant decreases in NDVI were mostly found in central and southwest TP [21]. They further found that increasing rates of vegetation greenness varied by land cover type [23]. In addition, there were large differences between results of the different datasets used to monitor the vegetation dynamics [24]. The influences of temperature and precipitation on vegetation growth vary substantially across the TP, especially in the arid and semi-arid regions [25]. In addition, since the 2000, a set of projects consisting of grazing exclusion and construction of national conservation areas, were carried out to protect and recover ecosystems degraded by high intensity grazing [26], [27]. Thus, it is necessary to examine vegetation development under the combined impacts of various natural factors and human activity.

Linear regression has been widely used to detect vegetation changes, focused primarily on changes in monotonic trends. Linear regression needs to be used with caution since any auto-correlation within the time series conflicts with model assumptions [28], and trends may be less significant than they appear [29]. Information regarding both positive and negative changes, for instance, are crucial for monitoring the effects of changes in land management or the influence of meteorological conditions on vegetation status. These positive and negative changes through time can be referred to as greening and browning, respectively. Monotonic changes may be

caused by gradual beneficial (positive) or adverse (negative) changes in external forces, while abrupt changes in a trend can be induced by a wide range of underlying processes that occur more quickly, These abrupt changes, or breakpoints, may be a result of sudden disturbances, such as wildfire or flood. In a water-limited environment (e.g., desert), vegetation grows quickly in response to heavy rainfall in a short period of time [30]. Abrupt changes may also be related to human disturbance activities [31]. In practice, there are promising methods focused on identifying abrupt changes in time series of remote sensing data [28], [32], [33]. Among these methods, the BFAST (Breaks For Additive Seasonal and Trend) method is extensively used because of its accuracy and its applicability in monitoring vegetation changes, urban extension, water body changes, etc [15].

A considerable number of studies have focused on exploring vegetation dynamics in this area, using long-term NDVI time series data from a number of remote sensing sensors, such as AVHRR or SPOT. Researchers explored specific components of time series such as the long-term trend, interannual cycle or seasonal behavior, whereas fewer studies focused on irregularities in the data. Most previous studies of long-term changes applied linear regression of annual NDVI to detect developing trends in vegetation growth [34]. However, the linear regression model is usually accompanied by the uncertainty that the fitted slope is not always significantly distinct from zero. We combined the Global Inventory Monitoring and Modeling Systems (GIMMS) NDVI3gV0 [12] dataset with an abrupt change point detection method to delineate the spatiotemporal dynamics of vegetation growth across the Tibetan Plateau (TP). A data-driven breakpoints detection approach capable of quantifying trend changes without prior knowledge of location or timing was utilized to explore vegetation changes on TP during 1982-2012.

II. MATERIALS AND METHODS

A. STUDY AREA

The Tibetan Plateau, known as the third pole on the Earth, has an average elevation of 4,500 meters and an area of about 2.5 million km^2, about one quarter of China territory (Figure 1) [35]. The plateau is located in a semi-arid/arid alpine climate zone with an annual precipitation of approximately 250 mm. Its precipitation varies with elevation, from 50-150mm in the southeast to 300-450 mm in the northwest. The plateau contains 11 types of vegetation cover, mainly consisting of shrub, steppe, meadow, and desert, which accounts for around three quarters of the total area.

B. DATASETS

1) GIMMS NDVI3G IMAGES

The primary dataset used in this analysis is the third-generation normalized difference vegetation index dataset (NDVI3g), released by NASA Global Inventory Monitoring and Modeling Systems (GIMMS). This dataset spans the
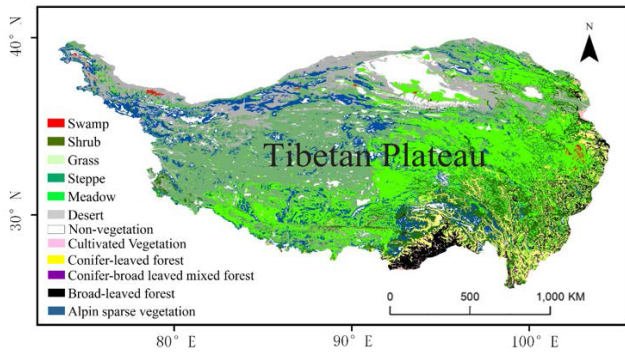
FIGURE 1. Map of vegetation cover types on the TP.

period from 1982 to 2012 with a spatial resolution of 0.083° and a temporal interval of 15 days [12], [36]. The GIMMS NDVI3g dataset, has been widely used in monitoring vegetation growth and dynamics from regional to continental scales [18]. It is the longest NDVI time series to date and has been proven to effectively monitor vegetation long-term dynamics [37]. In addition, the dataset has been normalized to account for issues such as sensor calibration loss, orbital drift, and atmospheric effects including those resulting from volcanic eruptions, so it can provide high quality data for regions from mid- to high-latitudes. Although the spatial resolution the NDVI3g dataset is relatively coarse, it is sufficiently detailed to explore vegetation change trend in this study area (2.5 million km^2). We extracted a temporal sequence of data for each pixel based on time series stacks of multi-temporal images. The Savitzky-Golay (S-G) smoothing filtering algorithm [38] was applied to further improve data consistency through time. Based on an analysis of the vegetation on the TP, an NDVI threshold value of 0.05 was set to exclude non-vegetated areas; pixels having a multi-year averaged NDVI less than the threshold value was set to null.

2) METEOROLOGICAL DATA

Temperature and precipitation raster data were obtained from the China meteorological forcing dataset created by merging data from a number of sources [9], [39]. These data sources include CMA (China Meteorological Administration) station records, TRMM (Tropical Rainfall Measuring Mission) satellite precipitation analysis data, Princeton forcing data, and GLDAS (Global Land Data Assimilation System) data. This dataset has a spatial and temporal resolution of 0.1 degree and 3-hours, respectively. It was then resampled to 8 km using the nearest neighbor method and aggregated monthly to match the GIMMS NDVI3g data. Figure 2 shows the spatial distribution of long-term trends for temperature and precipitation on the TP. The cooling trend in the northwestern part, and warming trend in southwestern part are both notable. In other areas, geographic distribution of cooling and warming trend is intermixed, as a result of the complex topography. There is a pronounced decrease in precipitation in the eastern TP, while evident increase in a large part of the western TP.
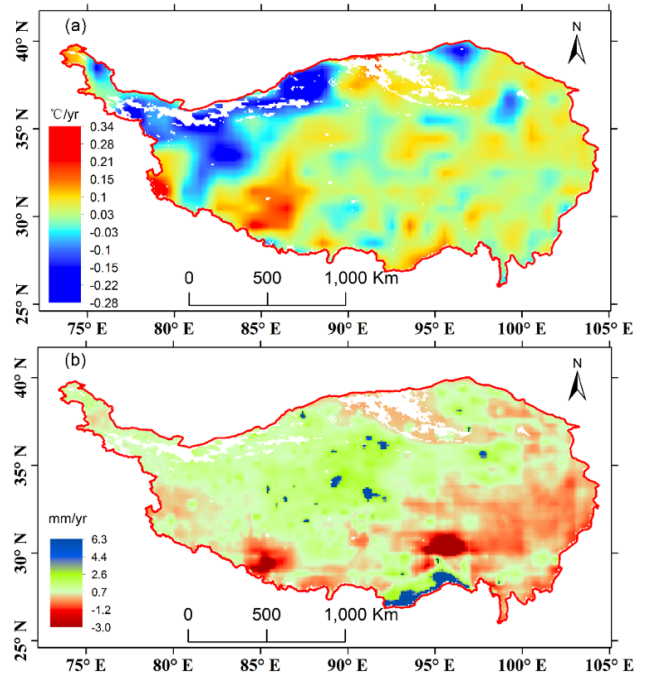

FIGURE 2. Long-term trends of monthly temperature (a) and precipitation (b) on the TP.

C. METHODS

A flowchart for the breakpoint analysis used in this paper is outlined in Figure 3. First, the GIMMS NDVI3g dataset was prepared for further analysis once outliers and noise were removed. Second, a seasonal-trend model was constructed using the R package 'BFAST' [29], [40] to determine the position of the breakpoint in each pixel. Third, vegetation was classified into one of eight trend types based on the
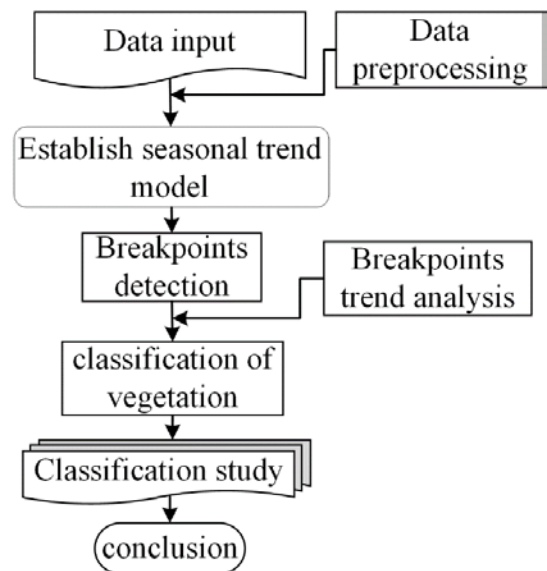

FIGURE 3. The flowchart for analyzing vegetation dynamics based on breakpoints.

vegetation growth trends on either side of the breakpoint. Finally, the spatiotemporal pattern of breakpoints and the trend types were further analyzed.

1) SEASONAL TREND ANALYSIS

To explain when and where the shift occurred in biological activity indicators after seasonal changes were accounted for, a seasonal-trend model was created based on the linear trend function and harmonic seasonal function (HSF) [40], [41]. Specifically, for an observations y_t at time t, the season-trend model is as follows:

$$y_t = y'_t + y^*_t + \varepsilon_t \qquad (1)$$

where

$$y'_t = \alpha + \beta t \qquad (2)$$

and

$$y^*_t = \sum_{j=1}^{k} \gamma_j \sin\left(\frac{2\pi jt}{f} + \delta_j\right)$$

where y'_t is the linear trend component and y^*_t simultaneously denotes a harmonic seasonal component; ε_t represents the residual error. In Equation 2, the intercept α, slope β ($\beta > 0$ indicates vegetative greening, while the converse indicates vegetative browning), amplitudes γ_j and phases δ_j are all unknown parameters, while f is the defined frequency (i.e., 24). This model takes complete account of both potential trends and seasonal variations in long-term data [42]. On this basis, the trend model shifts in each pixel as shown in the example in Figure 4).
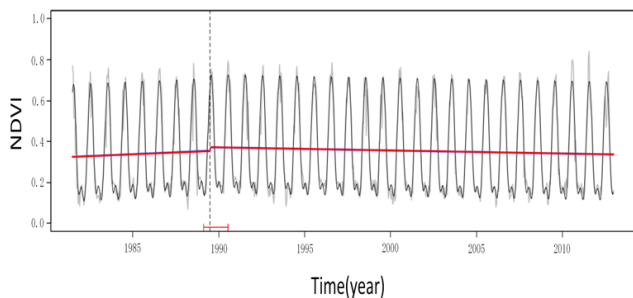

FIGURE 4. Major trend shift on the NDVI time series (gray curve) for a sample pixel. The season-trend model fitted curve is represented in black line. Red line indicates the growing trend, and downward red segment represents the confidence interval of change point timing.

2) BREAKPOINT DETECTION

Determining the existence of breakpoints, as well as their location, is a crucial step in the seasonal-trend model. The Moving Sums of Ordinary Least Square Residuals (OLS-MOSUM) method was applied to this dataset to detect breakpoints [42], [43]. If MOSUM detected a significant trend shift at any position, that position is considered to have a breakpoint in the data. The position of the breakpoints can also be solved by OLS techniques. The optimal number

of breakpoints was determined using Bayesian Information Criterion (BIC) [26], [44] as follows.

1) If OLS-MOSUM represents breakpoints in y'_t, the number and position of the breakpoints in the linear trend model are estimated from the data using $y'_t + \varepsilon_t$. Unknown parameters α and β were assessed using Robust Regression Analysis based on M-estimation. Each linear trend model can be estimated as Equation 2.

2) If the method of OLS-MOSUM represents the breakpoints in y^*_t, the number and position at the breakpoints in the harmonic seasonal model are estimated from the data $y^*_t + \varepsilon_t$. At this point, unknown parameters γ and δ were assessed using Robust Regression Analysis based on M-estimation. Each harmonic seasonal model can be estimated as Equation 3.

Repeat steps 1 and 2 until the number and position of breakpoints no longer change. At this point, final breakpoints are determined. In this study we focus on major trend shifts for each pixel that reflect the most important disturbances from natural or artificial influences.

3) TREND CLASSIFICATION BASED ON BREAKPOINTS

An abrupt change implies an obvious difference between the growth status before and after that change. To better interpret and understand the driving forces and ecological implications for these changes, we classified them in eight typical categories, which were defined as follows: two classes for monotonic trends, two categories for interrupted trends, and four classes representing trends with reversals on both sides of the breakpoint (Figure 5). Monotonic trends show that the vegetation has experienced greening or browning over time. Interrupted trends represent a plant greening or browning process that has been disturbed for some reason, resulting in
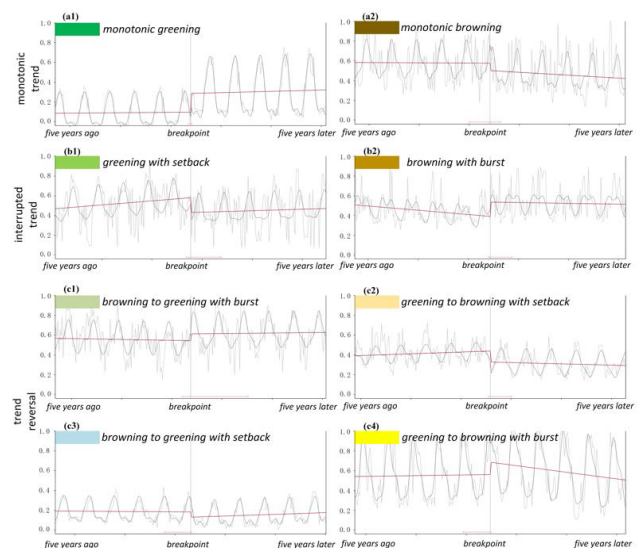

FIGURE 5. Vegetation changing types classified according the trends before and after breakpoints. To intuitively express the trend shifts information, the time series in these examples were limited to 10 years around the breakpoint dates.

a significant change. With trend reversals, growing processes are different on either side of the breakpoint.

The eight trend types are visualized in Figure 5. The first column shows that vegetation is greening (increasing NDVI) in recent years, whereas the second column represents vegetation browning (decreasing NDVI). The ecological characterization of trend shifts involves multiple change types, namely, continuous greening, continuous browning, browning to greening, and greening to browning. The abrupt changes between these types are identified by breakpoints. Pixels with a consistent trend (i.e., without substantial changes or identifiable breakpoints) were not considered in this study.

III. RESULTS
A. SPATIAL PATTERNS OF BREAKPOINTS
All eight trend types are characterized by a break in the long-term time series as noted by a change in the trend; the NDVI at the breakpoints may increase or decrease. By evaluating the temporal distribution, we found that the timing of breakpoints occurs most often during specific time periods. In other words, interannual variability in breakpoints is apparent (Table 1, Figure 6). Vegetation breakpoints span a broad time interval, which is concentrated in the mid-1990s but increases sharply in the period 2007-2010. The discrepancy in breakpoints distribution is pronounced; the maximum count of breakpoints (6709 in 2009-2010) is approximately 12 times higher than that of the minimum breakpoint count (559 in 1991-1992).

TABLE 1. Statistics of breakpoints number for every two years.

Year	1983–1984	1985–1986	1987–1988	1989–1990
count	2871	1120	1691	849
Year	1997–1998	1999–2000	2001–2002	2003–2004
count	1447	2422	2683	1987
Year	1991–1992	1993–1994	1995–1996	2005–2006
count	559	3534	2239	987
Year	2007–2008	2009–2010		
count	2254	6709		

Vegetation change points vary not only in time, but also in space. As shown in Figure 6, the spatial distribution of breakpoints is regional in nature, revealing the spatial heterogeneity of vegetation dynamic on the TP. The earliest trend shifts in the 1980s were mostly concentrated in the southeastern part of the TP, while trend shifts in the central TP occurred primarily during the 1990s (green). Trend shifts occurring after 2000 are widespread in the western and eastern parts of the TP. Compared with the 1980s, changing trends were identified for a larger region in the 1990s and 2000s. This reflects that relatively stable vegetation regimes have changed towards higher turnover rates, implying an increase in the complexity of environmental shifts and corresponding plant responses.
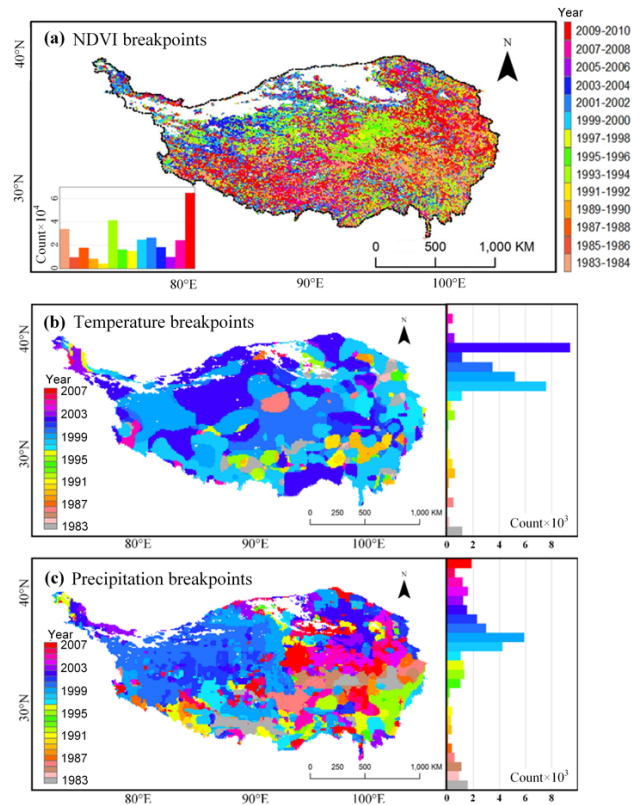

FIGURE 6. Spatial distribution of breakpoints in NDVI (a), temperature (b) and precipitation (c) on the TP, from 1982 to 2012.

B. SPATIAL DISTRIBUTION OF TREND MAGNITUDE
At the pixel level, the magnitude of the trends in vegetation was obtained from the slope coefficient in linear regression model (Figure 7). The spatial pattern suggests that statistically significant trends are positive for the vast majority of pixels, indicating the TP is becoming greener. Studies at the global scale have also confirmed that greening trends are more prevalent [4], [6], [34]. Browning trends in vegetation are rare on the TP with the exception of a small number of
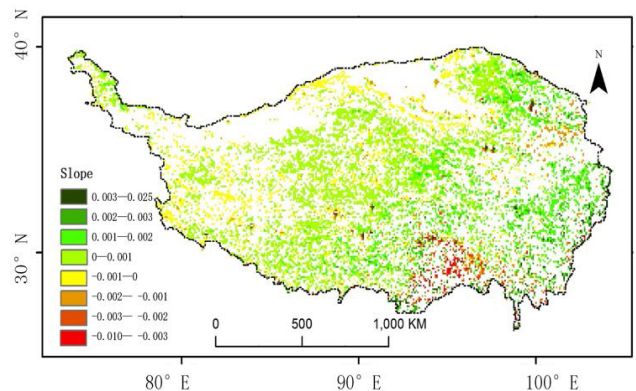

FIGURE 7. Spatial distribution of linear trend slopes on the TP for the period 1982-2012.

pixels located in the southern and northeastern areas. The magnitude of the trend is small, which may be the result of sparse vegetation cover and short growing seasons.

To quantify the detailed extent of change trend across the TP, we classified it into six categories according to the significant level of linear trend simulation (i.e., p value). Categories are first defined as three types: very small yet significant change, generally significant change and significant change. Then, greening and browning were taken into account. Thus, there are totally six categories to describe the degree of vegetation change. As presented in Table 2, the proportion of vegetation with a very small yet significant change toward greening (browning) is 33.38% (25.55%), indicating that most vegetation was stable during 1982-2012. The total proportion of greening vegetation is 59.97%, whereas browning vegetation accounts for 40.03%, again implying that the TP is generally becoming greener. Geographical regions where the vegetation changed significantly accounted for about one third of the TP, in which the proportions of vegetation greening and browning were 20.92% and 11.38%, respectively.

TABLE 2. Classification of vegetation linear trends according to trend signs and statistical significance.

Grands	slope	P value	pixels	proportion	total proportions
hardly significant greening	positive	[0.1,1)	11810	33.38%	
general significant greening	positive	[0.05,0.1]	2007	5.67%	greening：59.97%
significant greening	positive	(0,0.05]	7400	20.92%	
hardly significant browning	negative	[0.1,1)	9039	25.55%	
general significant browning	negative	[0.05,0.1]	1096	3.10%	browning：40.03%
significant browning	negative	(0,0.05]	4025	11.38%	

C. SPATIAL PATTERN OF TREND TYPE

After defining the eight trend types, their statistical and spatiotemporal distributions were investigated. A statistically significant level of 0.1 was chosen to identify pixels with a distinct vegetation growth trend on both sides of the break point (Table 3) to more thoroughly understand vegetation dynamics. Similar to the linear regression above for the entire NDVI time series, the statistically significant level of linear trends for each segment was fitted using pixel classification and piecewise regression. The type of greening or browning was determined by combining the linear trends of each segment at the breakpoints. Only pixels with a second segment showing an increasing (decreasing) trend was categorized as greening (browning). Under these conditions, the proportion of vegetation with greening and browning trends, was 46.78%

TABLE 3. Statistics of the greening and browning types mentioning the change points.

trend categories	trend types	pixels(p<0.1)	proportion	sum of proportions
monotonic trends	monotonic greening	492	2.32%	
interrupted trends	greening with setback	7352	34.74%	
Trend reversals	browning to greening with burst	1499	7.08%	greening：46.78%
trend reversals	browning to greening with setback	558	2.64%	
monotonic trends	monotonic browning	174	0.82%	
interrupted trends	browning with burst	4998	23.62%	
trend reversals	greening to browning with setback	2460	11.62%	browning：53.22%
trend reversals	greening to browning with burst	3631	17.16%	

and 53.22%, respectively. From this perspective, greening vegetation occurs slightly less often than browning vegetation when pixels with barely significant changes are excluded. The number of pixels with interrupted trends prevailed while there were fewer pixels with monotonic trends, which indicates that vegetation on the TP is frequently affected by changes in the environment.

The spatial pattern of vegetation growing trends exhibits a pronounced spatial heterogeneity, as shown in the map of trend type class (Figure 8). The majority of the pixels with significant change trend were discretely distributed across the TP. Greening with setback, the most common vegetation trend type, is primarily concentered in the central TP, with some pixels discretely distributed across the entire TP. Its spatial distribution in the central TP is consistent with that of breakpoints occurring during the period 1995-1998 (Figure 6). The second most common trend type, browning with burst, does not show a concentrated pattern. The other six types are all sparsely distributed across the TP, and no regular patterns are found. Monotonic trends, although showing a significant change in trend, account for the smallest percentage of the pixels and are not apparent on the map.

The statistical distribution also confirms that the trend type of greening with setback not only substantially contributes to the proportion of trend types, but also has change points located in a small temporal range, with a median
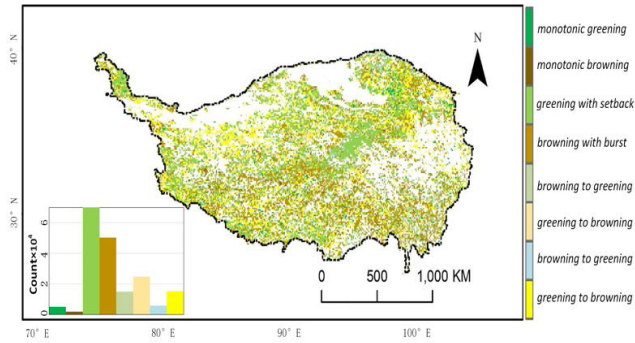
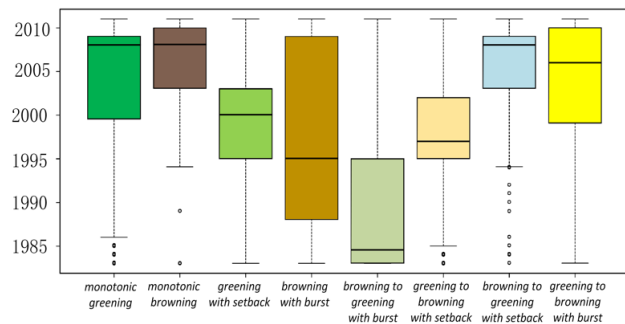**FIGURE 8.** Spatial distribution of the greening and browning types on the TP for the period 1982-2012.

FIGURE 9. Boxplots showing distribution of change years for each vegetation trend type.

FIGURE 10. Area proportion of various trend types in each vegetation cover.

value around the year 2000 (Figure 9). In contrast, change points for browning with burst are distributed across the largest time interval with a median in 1995. The trend type of browning to greening with burst has the smallest median value of change point, occurring in 1985 and implying that there were earlier greening trends of TP vegetation during the past three decades. The medians for monotonic greening and browning are close to the year 2010, as is the median for browning to greening with setback. These late change points can be confirmed by viewing the spatial distribution of change points around 2010 in Figure 6. Thus, the statistical and spatial distribution both suggest that the greening changes are generally interrupted with setback, followed by gradual browning with burst.

The proportion of every vegetation trend type that accounts for the total area in each vegetation cover was calculated and is shown in Figure 10. It is clear that in all vegetation cover types, the two vegetation trend types) greening with setback and browning with burst) occupy a substantial percentage of pixels. Approximately 80% of the vegetation in grasslands exhibits a browning growth trend with setback at the breakpoint. This browning with burst condition is followed by coniferous-leaved and coniferous-broad leaved mixed forest, with a percentage of ~30% each. Greening with setback is particularly striking in swamp, desert, steppe, and meadow regions, which account for about 40% of the land cover. Monotonic development trends in vegetation are minor
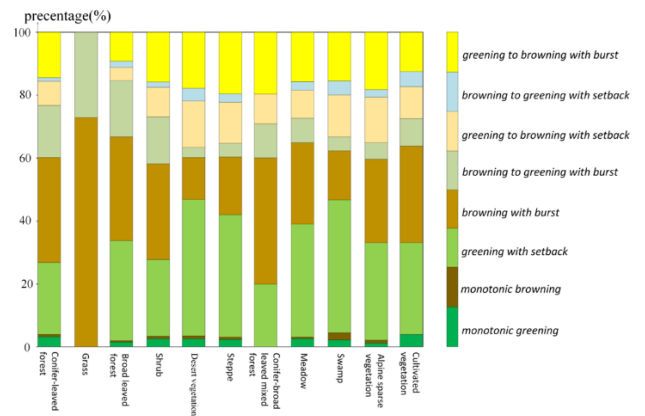
across all land covers, indicated by the small percentages of monotonic browning and greening trends. A small proportion of the land shows a trend for reversing changes between greening and browning. Among these trend types, greening to browning with burst takes a relatively strong position in areas with steppe, coniferous-broad leaved mixed forest, and alpine sparse vegetation. In contrast, browning to greening with setback is scarce across all vegetation types. Greening to browning with setback, on the other hand, accounts for approximately 10%~15% in most vegetation types, with the exception of grass, coniferous- and broad-leaved forest, and meadow.

IV. DISCUSSION

To understand the underlying factors influencing vegetation change on the Tibetan Plateau, both natural forces and human activities must be mentioned. Slowly acting environmental processes, including climate change, certain land management practices, or land degradation may cause gradual changes in a time series. The abrupt changes in vegetation may be attributed to extreme climatic events, such as droughts, heat waves, floods, and wildfires. Natural and anthropogenic effects are discussed next.

A. IMPACTS OF NATURAL FACTORS ON VEGETATION

Due to complex natural environments of the TP, vegetation dynamics may be significantly affected by natural factors. Temperature, precipitation, and solar radiation are the natural factors with the most control on vegetation growth on the TP [36]. In this study, only the direct impacts of temperature and precipitation on vegetation changes were considered. Solar radiation is strongly correlated with air temperature [45], so this discussion is still meaningful when it is not included. The significant warming and non-significant precipitation trends across the TP identified in this study agreed with findings in previous studies [14], [46]. Breakpoints in the time series of temperature and precipitation were calculated for each pixel using the methodology described

earlier (Figure 6b, 6c). According to the histogram (Figure 9a, right panel), breakpoints in temperature occurred mainly during the period 1997-2002. Change points in precipitation time series (Figure 6c) are mainly distributed in the period 1997-2007 and overlap with the temporal distribution of temperature breakpoints. Compared with temperature and precipitation breakpoints, vegetation breakpoints span a wider time window, which is not only concentrated in the mid-1990s, but is also distributed in the period 2007-2010. The relatively discrete vegetation breakpoints may result from the time-lag or memory effect of environmental factors on vegetation growth [47], [48]. In addition, compound effects from precipitation and temperature could lead to an irregular response in vegetation activity.

Spatially, precipitation breakpoints are more homogeneous than temperature breakpoints, which may be the result of complex topography and sparse rainfall. Most parts of TP show temperature breakpoints occurring in the 1990s, especially during the late 1990s (1997-1999), with the exception of the northeastern part and scattered patches in eastern, southern, and western parts. Regions with temperature change points in the 1980s cover a small patch in the southeastern part of the TP. Landscape heterogeneity in spatial distribution for precipitation breakpoints is prominent across the entire TP, demonstrated by a considerable number of small patches. In comparison with temperature, more precipitation breakpoints occur after the year 2000 in the eastern and southeastern regions.

The correlation of vegetation change points with those for temperature and precipitation were assessed by using their spatial distribution (Figure 6a vs. Figure 6b and 6c). For the entire TP, the Pearson correlation coefficient between change points in NDVI and temperature is 0.068, and that for NDVI and precipitation is 0.061. These very low correlations indicate that for the TP vegetation status shifts do not correspond with changes in temperature and precipitation. It should be noted that NDVI data has a temporal resolution of 15 days that may be too coarse to capture a sudden response of vegetation to abrupt changes in temperature or precipitation.

B. HUMAN INDUCED VEGETATION CHANGES

In addition to natural forces, human activity is a critical factor that can drive vegetation changes through land use management. Human disturbance on TP vegetation could primarily be attributed to the grazing restriction strategies of grassland designed by local and central policymakers. Since the 1990s, the government has implemented a series of policies that moved once-mobile herders into settlements and sharply limited livestock grazing. Local government, in particular, began to fence in grasslands under the fencing program. Pastures were planned at fixed locations within fixed areas to protect the grasslands that were over-grazed in the past. Most of the fenced grassland patches are distributed in the northern TP [49]. Previous studies reported that the fencing program has successfully improved the alpine grassland condition on the most degraded steppes but has not done as well on either

meadows or desert-steppes [50]. Jane and Qiu also confirm that the status of grasslands is far less healthy than reported, so it is urgent to understand how and why the pastures are changing [50]. In reality, the intensity of human interference is quite low, and pasture has been a traditional landscape for more than a thousand years [23], [49]. Thus, human activities would not be a dominant factor controlling vegetation changes. In this study, areas with vegetation showing greening trends, including persistent greening and greening with burst, are mainly located on the northern TP where desert grassland types are distributed. These areas were not affected by the fencing program. If this strategy worked, it would lead to improved vegetation condition, but our analyses indicates that the regions where vegetation show browning to greening trends are not found at northern fenced pastures.

In summary, it is difficult to attribute cause-and-effect to vegetation trend changes because variations in vegetation productivity are driven by various factors as shown in this study. Additionally, there may be errors in the NDVI3g dataset including platform changes between AVHRR satellites or orbital drift, which could induce trend shifts in NDVI time series. These effects have been effectively corrected as documented in previous studies [12]. The weak relationship of vegetation breakpoints with climatic changes may be induced by the complex response mechanism of plant to environmental shifts, such as compound changes in temperature, rainfall and soil moisture. The impacts of human activity may be primarily explained by gradual plant changes through time.

V. SUMMARY AND CONCLUSION

This study demonstrates that breakpoint detection and trend classification can effectively capture the spatiotemporal dynamics of vegetation activity on the TP. Greening and browning trends identified by the breakpoints are revealed across various biomes. The main conclusion is drawn as follows:

(1) The timing of change points are distributed across a time span rather than being concentrated at a specific time interval. Relatively, more breakpoints occur in the mid-1990s, the early 2000s and around 2010. Spatial distribution of breakpoints is also conspicuously heterogeneous. Central TP is dominated by the abrupt change points in vegetation trends that occurred around the year 1995. For other parts of the TP, the changes occurred mainly after the year 2000.

(2) Browning trends are barely noticeable in the western TP, although they are particularly evident in the southern and north-eastern parts. Vegetation in the central and eastern TP have enhanced greening trends. Most of the vegetation (about 58.93%) is growing in a stable status. The proportion for greening and browning vegetation is 59.97% and 40.03%, respectively. The geographical region where the vegetation changed significantly accounted for about 32.3% of TP total area.

(3) In the areas where vegetation are generally or significantly changed, vegetation greening is relatively

more common than vegetation browning in monotonic- and interrupted-trends, whereas browning trends was more conspicuous for reversal trend types than greening trends. Vegetation area with an interrupted trend (58.36%) is more prevalent than that with a monotonic trend (3.14%).

(4) The cause-effect analysis shows that vegetation trend changes on the TP cannot be attributed directly to climate change or human activities. This point is validated by the weak correlations between change points in NDVI, precipitation and temperature. This may be caused by long-term effects (e.g., time-lag effect) of climate variables on vegetation activity, or by low vegetation productivity on the TP.

REFERENCES

[1] R. Jong, J. Verbesselt, M. E. Schaepman, and S. Bruin, "Trend changes in global greening and browning: Contribution of short-term trends to longer-term change," *Global Change Biol.*, vol. 18, no. 2, pp. 642–655, Feb. 2012.

[2] A. M. Omer, "Energy, environment and sustainable development," *Renew. Sustain. Energy Rev.*, vol. 12, no. 9, pp. 2265–2300, Dec. 2008.

[3] S. Peng, "Benchmarking the seasonal cycle of CO_2 fluxes simulated by terrestrial ecosystem models," *Global Biogeochem. Cycles*, vol. 29, no. 1, pp. 46–64, 2015.

[4] R. R. Nemani, "Climate-driven increases in global terrestrial net primary production from 1982 to 1999," *Science*, vol. 300, no. 5625, pp. 1560–1563, Jun. 2003.

[5] R. M. Fuller, G. M. Smith, and B. J. Devereux, "The characterisation and measurement of land cover change through remote sensing: Problems in operational applications?" *Int. J. Appl. Earth Observ. Geoinformation*, vol. 4, no. 3, pp. 243–253, Jun. 2003.

[6] R. de Jong, S. de Bruin, A. de Wit, M. E. Schaepman, and D. L. Dent, "Analysis of monotonic greening and browning trends from global NDVI time-series," *Remote Sens. Environ.*, vol. 115, no. 2, pp. 692–702, Feb. 2011.

[7] W. Xu and X. Liu, "Response of vegetation in the Qinghai-Tibet Plateau to global warming," *Chin. Geograph. Sci.*, vol. 17, no. 2, pp. 151–159, Jun. 2007.

[8] Z. Xu, W. Liu, F. Li, and P. Liu, "Vegetation change and its relationship with precipitation on the southern Tibetan Plateau," *IAHS-AISH Proc. Rep.*, vol. 359, pp. 418–424, 2013.

[9] K. Yang, H. Wu, J. Qin, C. Lin, W. Tang, and Y. Chen, "Recent climate changes over the tibetan plateau and their impacts on energy and water cycle: A review," *Global Planet. Change*, vol. 112, pp. 79–91, Jan. 2014.

[10] M. H. Xu, M. Liu, D. T. Zhai, X. Xue, F. Peng, and Q. G. You, "Dynamic changes in biomass and its relationship with environmental factors in an alpine meadow on the Qinghai-Tibetan Plateau, based on simulated warming experiments," *Shengtai Xuebao/Acta Ecol. Sin.*, vol. 36, no. 18, pp. 5759–5767, 2016.

[11] W. Qiji, J. Zengchun, W. Wenying, L. Baining, M. Yushou, and J. Weiping, "The study of grassland resource, ecological enviroment and sustainable developent in Qinghai–Xizang Plateau," *Qinghai Prataculture*, vol. 6, no. 3, pp. 1–11, 1997.

[12] J. E. Pinzon and C. J. Tucker, "A non-stationary 1981–2012 AVHRR NDVI3g time series," *Remote Sens.*, vol. 6, no. 8, pp. 6929–6960, 2014.

[13] A. Anyamba, J. L. Small, C. J. Tucker, and E. W. Pak, "Thirty-two years of Sahelian zone growing season non-stationary NDVI3g patterns and trends," *Remote Sens.*, vol. 6, no. 4, pp. 3101–3122, 2014.

[14] J. Tao, Y. Zhang, J. Dong, Y. Fu, J. Zhu, G. Zhang, Y. Jiang, L. Tian, X. Zhang, T. Zhang, and Y. Xi, "Elevation-dependent relationships between climate change and grassland vegetation variation across the Qinghai-Xizang Plateau," *Int. J. Climatol.*, vol. 35, no. 7, pp. 1638–1647, Jun. 2015.

[15] G. Zhang, Y. Zhang, J. Dong, and X. Xiao, "Green-up dates in the tibetan plateau have continuously advanced from 1982 to 2011," *Proc. Nat. Acad. Sci. USA*, vol. 110, no. 11, pp. 4309–4314, Mar. 2013.

[16] L. Zhou, C. J. Tucker, R. K. Kaufmann, D. Slayback, N. V. Shabanov, and R. B. Myneni, "Variations in northern vegetation activity inferred from satellite data of vegetation index during 1981 to 1999," *J. Geophys. Res., Atmos.*, vol. 106, no. D17, pp. 20069–20083, Sep. 2001.

[17] M. Du, "Mutual influence between human activities and climate change in the tibetan plateau during recent years," *Global Planet. Change*, vol. 41, nos. 3–4, pp. 241–249, Jul. 2004.

[18] R. de Jong, J. Verbesselt, A. Zeileis, and M. Schaepman, "Shifts in global vegetation activity trends," *Remote Sens.*, vol. 5, no. 3, pp. 1117–1133, 2013.

[19] N. Pan, X. Feng, B. Fu, S. Wang, F. Ji, and S. Pan, "Increasing global vegetation browning hidden in overall vegetation greening: Insights from time-varying trends," *Remote Sens. Environ.*, vol. 214, pp. 59–72, Sep. 2018.

[20] C. Chen, T. Park, X. Wang, S. Piao, B. Xu, R. K. Chaturvedi, R. Fuchs, V. Brovkin, P. Ciais, R. Fensholt, H. Tømmervik, G. Bala, Z. Zhu, R. R. Nemani, and R. B. Myneni, "China and India lead in greening of the world through land-use management," *Nature Sustainability*, vol. 2, no. 2, pp. 122–129, Feb. 2019.

[21] L. Zhang, H. Guo, L. Ji, L. Lei, C. Wang, D. Yan, B. Li, and J. Li, "Vegetation greenness trend (2000 to 2009) and the climate controls in the qinghai-tibetan plateau," *J. Appl. Remote Sens.*, vol. 7, no. 1, Apr. 2013, Art. no. 073572.

[22] D. Chu, L. Lu, and T. Zhang, "Sensitivity of normalized difference vegetation index (NDVI) to seasonal and interannual climate conditions in the Lhasa area, Tibetan plateau, China," *Arctic, Antarctic, Alpine Res.*, vol. 39, no. 4, pp. 635–641, Nov. 2007.

[23] K. Huang, Y. Zhang, J. Zhu, Y. Liu, J. Zu, and J. Zhang, "The influences of climate change and human activities on vegetation dynamics in the Qinghai-Tibet Plateau," *Remote Sens.*, vol. 8, no. 10, p. 876, 2016.

[24] Y. Zhang, C. Song, L. E. Band, G. Sun, and J. Li, "Reanalysis of global terrestrial vegetation trends from MODIS products: Browning or greening?" *Remote Sens. Environ.*, vol. 191, pp. 145–155, Mar. 2017.

[25] C. Huang, Y. Li, G. Liu, H. Zhang, and Q. Liu, "Recent climate variability and its impact on precipitation, temperature, and vegetation dynamics in the Lancang River headwater area of China," *Int. J. Remote Sens.*, vol. 35, no. 8, pp. 2822–2834, Apr. 2014.

[26] J. Wu, Y. Feng, X. Zhang, S. Wurst, B. Tietjen, P. Tarolli, and C. Song, "Grazing exclusion by fencing non-linearly restored the degraded alpine grasslands on the tibetan plateau," *Sci. Rep.*, vol. 7, no. 1, Dec. 2017, Art. no. 15202.

[27] G. Xu, "Effect of grazing disturbance on species diversity of alpine grassland plant community in Eastern Qilian Mountains," *J. Gansu Agric. Univ.*, vol. 6, pp. 789–796, 2005.

[28] J. Verbesselt, R. Hyndman, G. Newnham, and D. Culvenor, "Detecting trend and seasonal changes in satellite image time series," *Remote Sens. Environ.*, vol. 114, no. 1, pp. 106–115, Jan. 2010.

[29] J. Verbesselt, R. Hyndman, A. Zeileis, and D. Culvenor, "Phenological change detection while accounting for abrupt and gradual trends in satellite image time series," *Remote Sens. Environ.*, vol. 114, no. 12, pp. 2970–2980, Dec. 2010.

[30] M. J. B. Zeppel, J. V. Wilks, and J. D. Lewis, "Impacts of extreme precipitation and seasonal changes in precipitation on plants," *Biogeosciences*, vol. 11, no. 11, pp. 3083–3093, 2014.

[31] J. Eastman, F. Sangermano, E. Machado, J. Rogan, and A. Anyamba, "Global trends in seasonality of normalized difference vegetation index (NDVI), 1982–2011," *Remote Sens.*, vol. 5, no. 10, pp. 4799–4818, 2013.

[32] R. E. Kennedy, Z. Yang, and W. B. Cohen, "Detecting trends in forest disturbance and recovery using yearly Landsat time series: 1. LandTrendr—Temporal segmentation algorithms," *Remote Sens. Environ.*, vol. 114, no. 12, pp. 2897–2910, 2010.

[33] C. Huang, S. N. Goward, J. G. Masek, N. Thomas, Z. Zhu, and J. E. Vogelmann, "An automated approach for reconstructing recent forest disturbance history using dense Landsat time series stacks," *Remote Sens. Environ.*, vol. 114, no. 1, pp. 183–198, Jan. 2010.

[34] Z. G. Bai, D. L. Dent, L. Olsson, and M. E. Schaepman, "Proxy global assessment of land degradation," *Soil Use Manage.*, vol. 24, no. 3, pp. 223–234, Sep. 2008.

[35] T. Yao, F. Wu, L. Ding, J. Sun, L. Zhu, S. Piao, T. Deng, X. Ni, H. Zheng, and H. Ouyang, "Multispherical interactions and their effects on the tibetan Plateau's Earth system: A review of the recent researches," *Nat. Sci. Rev.*, vol. 2, no. 4, pp. 468–488, Dec. 2015.

[36] D. Peng, B. Zhang, L. Liu, D. Chen, H. Fang, and Y. Hu, "Seasonal dynamic pattern analysis on global FPAR derived from AVHRR GIMMS NDVI," *Int. J. Digit. Earth*, vol. 5, no. 5, pp. 439–455, Sep. 2012.

[37] D. Stow, S. Daeschner, A. Hope, D. Douglas, A. Petersen, R. Myneni, L. Zhou, and W. Oechel, "Variability of the seasonally integrated normalized difference vegetation index across the north slope of Alaska in the 1990s," *Int. J. Remote Sens.*, vol. 24, no. 5, pp. 1111–1117, Jan. 2003.

[38] J. Chen, P. Jönsson, M. Tamura, Z. Gu, B. Matsushita, and L. Eklundh, "A simple method for reconstructing a high-quality NDVI time-series data set based on the Savitzky–Golay filter," *Remote Sens. Environ.*, vol. 91, nos. 3–4, pp. 332–344, 2004.

[39] K. Yang, B. Ye, D. Zhou, B. Wu, T. Foken, J. Qin, and Z. Zhou, "Response of hydrological cycle to recent climate changes in the tibetan plateau," *Climatic Change*, vol. 109, nos. 3–4, pp. 517–534, Dec. 2011.

[40] J. Verbesselt, A. Zeileis, and M. Herold, "Near real-time disturbance detection using satellite image time series," *Remote Sens. Environ.*, vol. 123, pp. 98–108, Aug. 2012.

[41] C. Potter, P.-N. Tan, M. Steinbach, S. Klooster, V. Kumar, R. Myneni, and V. Genovese, "Major disturbance events in terrestrial ecosystems detected using global satellite data sets," *Global Change Biol.*, vol. 9, no. 7, pp. 1005–1021, Jul. 2003.

[42] A. Zeileis, F. Leisch, K. Hornik, and C. Kleiber, "Strucchange: AnRPackage for testing for structural change in linear regression models," *J. Stat. Softw.*, vol. 7, no. 2, pp. 1–38, 2002.

[43] X. Zhang, M. A. Friedl, C. B. Schaaf, A. H. Strahler, J. C. F. Hodges, F. Gao, B. C. Reed, and A. Huete, "Monitoring vegetation phenology using MODIS," *Remote Sens. Environ.*, vol. 84, no. 3, pp. 471–475, Mar. 2003.

[44] A. Zeileis and C. Kleiber, "Validating multiple structural change models—A case study," *J. Appl. Econometrics*, vol. 20, no. 5, pp. 685–690, Jul. 2005.

[45] K. L. Bristow and G. S. Campbell, "On the relationship between incoming solar radiation and daily maximum and minimum temperature," *Agricult. Forest Meteorol.*, vol. 31, no. 2, pp. 159–166, May 1984.

[46] J. Liu, S. Wang, S. Yu, D. Yang, and L. Zhang, "Climate warming and growth of high-elevation inland lakes on the tibetan plateau," *Global Planet. Change*, vol. 67, nos. 3–4, pp. 209–217, Jun. 2009.

[47] D. Wu, X. Zhao, S. Liang, T. Zhou, K. Huang, B. Tang, and W. Zhao, "Time-lag effects of global vegetation responses to climate change," *Global Change Biol.*, vol. 21, no. 9, pp. 3520–3531, Sep. 2015.

[48] R. K. Kaufmann, L. Zhou, R. B. Myneni, C. J. Tucker, D. Slayback, N. V. Shabanov, and J. Pinzon, "The effect of vegetation on surface temperature: A statistical analysis of NDVI and climate data," *Geophys. Res. Lett.*, vol. 30, no. 22, Nov. 2003.

[49] R. J. Long, L. M. Ding, Z. H. Shang, and X. H. Guo, "The yak grazing system on the qinghai-tibetan plateau and its status," *Rangeland J.*, vol. 30, no. 2, pp. 241–246, 2008.

[50] J. Qiu, "Trouble in Tibet," *Nature*, vol. 529, no. 7585, pp. 142–145, Jan. 2016.

YONG NI was born in Zaozhuang, Shandong, China, in 1988. He received the M.S. degree in cartography and geographic information system from the Institute of Geographical Sciences and Natural Resources Research, Chinese Academy of Sciences, Beijing, China, in 2014.

He is currently an Engineer with the Department of Environment Quality Comprehensive Assessment, China National Environmental Monitoring Center. His research interests include designing, construction, and management of the ecological environment monitoring information networks, designation of the data standard, and opening and sharing of environmental monitoring data.

YUKE ZHOU was born in Jining, Shandong, China, in 1984. He received the Ph.D. degree in cartography and geographic information system from the Institute of Geographical Sciences and Natural Resources Research, Chinese Academy of Sciences, Beijing, China, in 2013.

He is currently an Assistant Researcher with the Institute of Geographical Sciences and Natural Resources Research, CAS. His research interests include remote sensing applications in climate changes and ecosystem monitoring.

JUNFU FAN was born in Liaocheng, Shandong, China, in 1985. He received the B.S. and M.S. degrees in cartography and geographic information system from the Shandong University of Science and Technology, Qingdao, China, in 2008 and 2011, respectively, and the Ph.D. degree in cartography and geographic information system from the Institute of Geographical Sciences and Natural Resources Research, Chinese Academy of Sciences, Beijing, China, in 2014.

He is currently a Lecturer with the Department of Surveying and Mapping Engineering, Shandong University of Technology. His research interests include high performance geo-computing, spatial analysis algorithm design and development, and remote sensing of urban environment.

• • •